Priyabrata Mohapatra[1] / **Mayank Mittal**[1]

A Simplified One-Dimensional Mathematical Model to Study the Transient Thermal Behavior of an Oxidation Catalyst with Both Low and High Levels of CO Concentration at the Inlet

[1] Department of Mechanical Engineering, Indian Institute of Technology Madras, Chennai, Tamil Nadu 600036, India, E-mail: me15s025@smail.iitm.ac.in, mmittal@iitm.ac.in

Abstract:
In recent years, the permissible limits of engine exhaust emissions are reduced considerably. Hence a quick warm-up and high conversion efficiency of the catalyst system is essential to meet upcoming stringent emission regulations. In the present work, the transient thermal behavior of an oxidation catalyst is studied using a one-dimension mathematical modeling approach with the focus on CO oxidation for dual-fuel engine application. At first, the heat generation due to chemical reactions is considered negligible for studying the warm-up behavior. Upon obtaining a good agreement between predicted warm-up temperature profiles with available literature data, the effect of an electrical heater on the warm-up behavior is investigated. The model is then extended by incorporating heat generation due to CO oxidation. A simplified reaction rate model is considered in order to reduce the computational complexity. It is observed that the simplified model agrees well with the experimental data for both low and high levels of CO concentration at the inlet, typical in dual-fuel technology when an engine is operated under diesel and dual-fuel modes, respectively.

Keywords: mathematical modeling, catalytic converter, CO oxidation, heat and mass transfer, reaction model, dual-fuel engine

DOI: 10.1515/cppm-2018-0049

Received: August 27, 2018; **Revised:** November 11, 2018; **Accepted:** December 5, 2018

1 Introduction

Over the last several years, automotive emission regulations have become more and more stringent due to growing concerns over air pollution and potential health hazards such as respiratory and cardiovascular diseases. The first emission control program started in 1970 by California Air Control Board (CARB), which is considered to be the beginning of emission control era. Compared to gasoline engines, diesel engines produce lesser carbon monoxide (CO) and hydrocarbon (HC) emissions [1], however, nitrogen oxides (NO_x) and particulate matter (PM) are still a serious concern. NO_x is formed mainly due to high in-cylinder temperature during combustion and availability of oxygen due to overall lean mixture [2, 3]. PM is defined as any matter in the exhaust gas of an internal combustion engine that can be trapped on a sampling medium at 325 K or less [1]. It is broadly classified into three major categories, known as dry carbon or soot, inorganic oxides and soluble organic fractions. Dry soot arises due to heterogeneous combustion, where local equivalence ratio exceeds more than two [2]. NO_x in the atmosphere reacts with hydrocarbons to form photochemical smog and acid rains. Moreover, NO_x and PM are alarming human hazards. These pollutants affect human respiratory system, damages lung tissues and causes bronchitis, etc [4]. Also, one of the major concerns in both gasoline and diesel engines is the cold start emissions, as this alone contributes up to about 80 % of total HC and CO emissions during the whole transient cycle. During this cold transient cycle, in order to start and sustain the combustion, relatively rich fuel-air mixture is supplied to the combustion chamber, which causes increase in fuel consumption and exhaust emissions [5]. Note that the efficency of a three-way catalytic converter is also low during the cold start due to low exhaust gas temperature and rich fuel-air ratio [6].

Though, many different approaches such as exhaust gas recirculation, in-cylinder strategies, for example, control of injection timing and number of injections, along with optimization of combustion chamber geometry

Mayank Mittal is the corresponding author.

have been used to reduce the engine-out emissions, it is still difficult to meet upcoming stringent emission regulations. It is to be noted that alternative fuel technologies, for example, dual-fuel technology, in which natural gas acts as a primary fuel and ignited by a pilot quantity of diesel [7], produces significantly lesser NO_x and PM compared to diesel only operation [8, 9]. However, during low and moderate loads, due to lower combustion efficiency, there is a significant increase in hydrocarbons (mostly methane) and CO [10]. For instance, an engine operating under dual fuel mode produces high level of CO (250 ppm to 2500 ppm) compared to CO levels (10 ppm to 500 ppm) when operated under diesel only mode [11, 12]. Hence, an oxidation catalyst with high conversion efficiency is essential for dual-fuel engine technology.

A diesel oxidation catalyst consists of a monolith substrate (metallic or ceramic) encased in a stainless steel housing. The monolith substrate generally has a large number of channels to provide a large surface area to volume ratio, and also increases the residence time of the flow [13]. A washcoat such as alumina is then applied on the walls of the channels which acts as a support system for carrying the catalysts (for example, platinum, palladium, etc.), and also provides an increase in the surface area for depositing the catalyst material. The performance of the catalyst system, however, depends on various factors such as substrate material, channel design, type of catalyst and its loading, and so on. Designing a catalyst system solely on the basis of experimental iterations is generally not a feasible option because of time and cost restrictions. Hence, a predictive mathematical model based on underlying physical and chemical phenomena plays a vital role to perform parametric studies and optimise the overall system design. However, a three-dimensional modeling of the entire catalyst system is computationally very expensive, and thus, practically impossible. Instead, a one-dimensional mathematical modeling is a viable choice with global rate reactions that describes the phenomenon in the catalytic converter reasonably well with low computational efforts, and provides useful information for quick design iterations. A first step towards the simplification of modeling efforts is to reduce the three-dimensional coordinates into two-dimensional coordinates (i. e. axial and radial). A further simplification to one-dimensional coordinate (i. e. axial) is ensured by neglecting the effects of radial heat conduction. This allows the entire catalyst to be modeled with only one channel by utilizing average flow parameters, neglecting channel's mal-distribution. The effects of surface adsorption-desorption and pore diffusion through the washcoat are often neglected, and essentially lumped into the kinetic rate expressions of global reaction rate models [13]. As the efficiency of a catalyst system depends upon chemical species, temperature and residence time, the entire catalyst can be modeled using species and energy conservation equations considering two phases, i. e. bulk gas and surface. It is worth notifying that the momentum equation is often neglected in the modeling efforts because the pressure throughout the catalyst is essentially constant. The equations of species conservation keep track of species concentrations in the bulk gas and at the surface of the channel. However, the presence of a large number of reactions still makes the modeling efforts computationally expensive, and requires further simplification. The energy conservation equations provide the temperature profiles for both bulk gas and surface through the catalyst.

In the present work, a simplified one-dimensional mathematical model is developed to study the transient thermal behavior of an oxidation catalyst. As NO_x and PM can be simultaneously reduced in dual-fuel engine application, and that the major constituent of HC is methane which has slow oxidation [14, 15] and does not come under non-methane hydrocarbon (NMHC) regulations during on-board diagnostics (OBD) [16], the focus is laid upon CO oxidation. During warm-up, as there is no appreciable chemical reaction that takes place at the surface of the catalyst, the model is first considered without heat generation and validated with [17]. Later, the model is extended to incorporate the CO oxidation with simplified reaction rate model for studying the light-off behavior, and validated with low level of CO concentration with available experimental data from [18]. The simplified model is also validated for the case with high level of CO concentration (typical in dual-fuel engines) with [19, 20] for the applicability of the model over a wide range of CO concentration at the inlet of the catalyst system.

2 Mathematical model to study the warm-up behavior of the catalytic converter

At first, the mathematical model only on the basis of energy conservation equations is considered to study the warm-up behavior of the catalytic converter. This provides the model a greater utility by not restricting it to a particular catalyst system for warm-up studies. Eq. (1) and (2) represent to energy conservations for bulk gas and surface, respectively.

$$\varepsilon\, k_g \frac{\partial}{\partial x}\left(\frac{\partial T_g}{\partial x}\right) - G\, C_{pg}\frac{\partial T_g}{\partial x} - a_s h\left(T_g - T_s\right) = \varepsilon\, \rho_g C_{pg}\frac{\partial T_g}{\partial t} \tag{1}$$

$$(1-\varepsilon)\,k_s\frac{\partial}{\partial x}\left(\frac{\partial T_s}{\partial x}\right)+a_s h\left(T_g-T_s\right)=(1-\varepsilon)\,\rho_s C_s\frac{\partial T_s}{\partial t} \tag{2}$$

where, k_g [J/ (m · s · K)] and k_s[J/ (m · s · K)] are the thermal conductivities of bulk gas and solid, respectively. ε [-] is the void fraction, T_g [K] is the bulk gas temperature, T_s [K] is the surface (or monolith) temperature, C_{pg} [J/(kg · K)] is the specific heat of gas at constant pressure, C_s [J/(kg · K)] is the specific heat of solid, x [m] is the axial distance, h $\left[\mathrm{J/\left(m^2\cdot s\cdot K\right)}\right]$ is the heat transfer coefficient between gas and solid, a_s $\left[\mathrm{m^2/m^3}\right]$ is the geometric surface area per unit reactor volume, ρ_s $\left[\mathrm{kg/m^3}\right]$ and ρ_g $\left[\mathrm{kg/m^3}\right]$ are the densities of solid and bulk gas, respectively. G $\left[\mathrm{kg/\left(m^2\cdot s\right)}\right]$ is the rate of mass flow of gas, and t [s] represents to the time. The first term on the left-hand side of eq. (1) represents to the axial heat conduction in the bulk gas, the second term represents to the enthalpy transfer due to bulk motion, and the third term describes the convective heat transfer between bulk gas and surface. The term on the right-hand side of eq. (1) represents to energy accumulation in the bulk gas. Similarly, the first term on the left-hand side of eq. (2) represents to the axial heat conduction in surface, and the second term represents to the convective heat transfer between bulk gas and surface. The term on the right-hand side of eq. (2) describes the energy storage for the surface. The accumulation and axial heat conduction terms in the bulk gas energy equation, eq. (1), however, are neglected as they are very small compared to other terms [17]. The absence of accumulation term also makes the catalyst modeling easier, and thus, avoids the numerical difficulties. The axial conduction term in the surface phase energy equation [eq. (2)] is also neglected, as it is found to be much smaller compared to convective heat transfer and storage terms of the monolith [17]. After above assumptions, eqs. (1) and (2) can be written as;

$$\frac{\partial T_g}{\partial z}+\frac{a_s hL}{GC_{pg}}\left(T_g-T_s\right)=0 \tag{3}$$

$$\frac{\partial T_s}{\partial t}=\frac{a_s h}{(1-\varepsilon)\,\rho_s C_s}\left(T_g-T_s\right) \tag{4}$$

where, $\Delta z=\Delta x/L$, i. e. normalized axial distance. In many converter designs, space velocity $\left(\sigma,\left[\mathrm{hr^{-1}}\right]\right)$ is one of the important factors for consideration. In a heterogeneous fixed-bed catalyst, the residence time is defined in terms of volumetric flow and volume of the catalyst [1]. Space velocity, eq. (5), is calculated usually on the basis of outside physical dimensions. The volumetric gas flow rate is generally considered at standard temperature and pressure (STP).

$$\text{space velcoity}\,(\sigma)=\frac{\text{volume flow rate of feed at STP}}{\text{physical volume of the catalyst}} \tag{5}$$

Therefore, eq. (3) can also be re-written as;

$$\frac{\partial T_g}{\partial z}+\left(\frac{a_s h}{GC_{pg}}\right)\left(\frac{G}{\sigma\rho_{STP}}\right)\left(T_g-T_s\right)=0 \tag{6}$$

here, space velocity and bulk gas density $\left(\rho_{STP}\,[kg/m^3]\right)$ are calculated at the STP condition. The local heat transfer coefficient (h) and specific heat of gas $\left(C_{pg}\right)$ are considered from Vardi and Biller [17]. The average bed temperature of the solid is:

$$T_{av}(t)=\frac{\int_0^1 T_s\,(t,\,z)dz}{\int_0^1 dz=\int_0^1 T_s(t,\,z)dz} \tag{7}$$

The surface phase energy equation [eq. (4)] is discretized using the forward difference method, while the energy equation for the bulk gas [eq. (6)] is discretized using the backward difference method. Note that the central difference method is not used due to restrictions imposed on both time step and axial interval. Therefore,

$$T_{s,i}^{n+1}=\left(1-\frac{ha_s}{(1-\varepsilon)\rho_s C_s}\Delta t\right)T_{s,i}^{n}+\left(\frac{ha_s}{(1-\varepsilon)\rho_s C_s}\Delta t\right)T_{g,i}^{n} \tag{8}$$

$$T_{g,i}^{n+1} = \frac{T_{g,i-1}^{n+1} + \left(\frac{ha_s\Delta z}{C_{pg}\ \sigma\ \rho_{STP}}\right) T_{s,i}^{n+1}}{1 + \left(\frac{ha_s\Delta z}{C_{pg}\ \sigma\ \rho_{STP}}\right)} \tag{9}$$

where, $n + 1$ represents to the temperature at time $t + \Delta t$, and i represents to the axial node of the converter. Here, the time step restriction is:

$$\Delta t \leq \frac{(1-\varepsilon)\,\rho_s C_s}{a_s h} \tag{10}$$

The warm-up model is validated for the converter of length 0.42 m (1.38 ft) with mass flow rate of 1.36 kg/m^2.s (1000 lb./sq.ft.hr), and geometric surface area of 984.25 m^2/m^3 (300 sq.ft/cu.ft). A detailed information of various converter parameters are provided in Table 1.

Table 1: Parameters for validating the warm-up behavior of the catalytic converter [17].

Symbol	Parameter	Quantity
σ	space velocity	10,000 hr^{-1}
L	length of monolith	0.42 m (1.38 ft)
Pr	Prandtl number	0.73
Ψ	shape factor for catalyst particles	0.91
G	mass flow rate of gas	1.36 kg/(m^2·s) (1000 lb/(ft^2·hr))
a_s	geometric surface area per unit reactor volume	984.25 m^2/m^3 (300 ft^2/ft^3)
T_{s0}	initial temperature of solid	299.8 K (80°F)
T_{g0}	inlet steady-state temperature of bulk gas	899.8 K (1160°F)
$(1–\varepsilon)\rho_s$	effective solid density	830 kg/m^3

Figure 1 shows the comparison of average bed temperature with available data from [17]. Transient temperature profiles for both bulk gas and solid are also plotted approximately for every 0.76 minute (see Figure 2). Note that the maximum reachable temperature in the above case is 899.8 K (or 1160 °F), which is mainly due to the absence of the source term. As expected, simulated temperature profiles of both bulk gas and solid are close to each other [17]. This is mainly due to small size of the catalyst pellets used, and availability of large surface area, approximately 984.25 m^2/m^3 (300 sq.ft/cu.ft), hence a small resistance for the heat transfer between the bulk gas and the solid. This type of analysis is particularly useful to estimate the transient temperature distribution during warm-up and for the preliminary design of converter without depending upon a particular catalyst system.

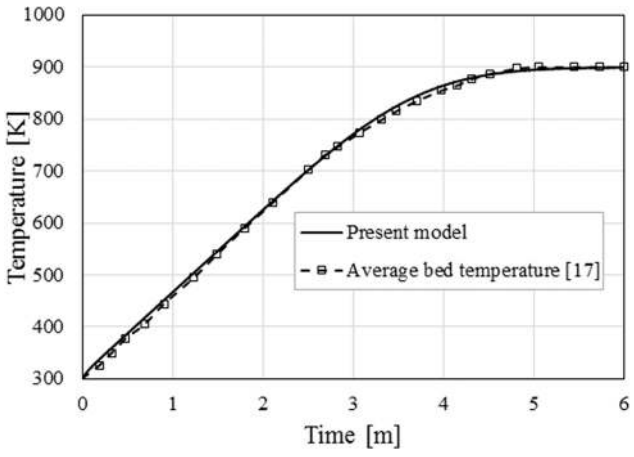

Figure 1: Comparison of average bed temperature of the solid between present model literature data.

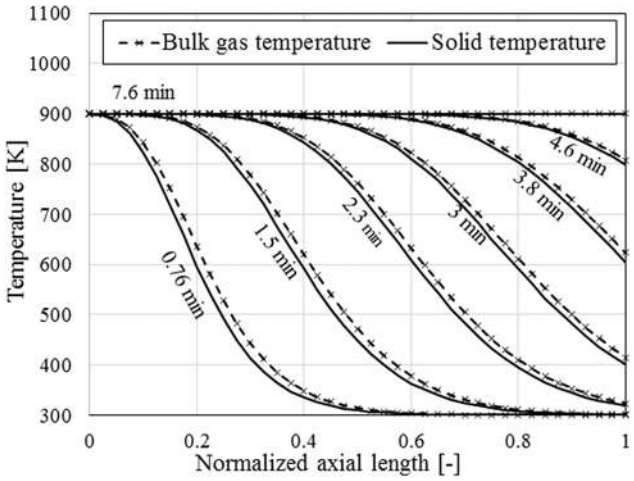

Figure 2: Comparison between computed bulk gas and solid temperature profiles.

Effect of external heater during the warm-up period of the converter:

During the warm-up period, as there is no appreciable heat generation, an external electrical heater can be employed, thus improving the transient thermal behavior of the converter. Hence a supplementary resistive heat source term (P/V_x) is introduced in the energy equation of the solid phase [eq. (10)], where P [W] is the power supply, and V_x $\left[\mathrm{m}^3\right]$ is the volume of the monolith selected for the heating purpose.

$$(1-\varepsilon)\,\rho_s C_s \frac{\partial T_s}{\partial t} = (1-\varepsilon)\,k_s \frac{\partial}{\partial x}\left(\frac{\partial T_s}{\partial x}\right) + a_s h\left(T_g - T_s\right) + \frac{P}{V_x} \tag{11}$$

Note that $0 \le V_x \le V_m$, where V_m $\left[\mathrm{m}^3\right]$ is the total volume of the converter (monolith), provides a uniform heating for the heated zone and zero heating for the non-heated zone. This gives the flexibility to the user utilizing an external heater for a given converter volume. However, in the present work, the external heater is applied to the whole converter volume to evaluate its influence during the warm-up condition.

The discretized version of the surface energy equation, eq. (11), with the source term is following,

$$T_{s,i}^{n+1} = \left(1 - \frac{h a_s}{(1-\varepsilon)\,\rho_s C_s}\Delta t\right) T_{s,i}^{n} + \left(\frac{h a_s}{(1-\varepsilon)\,\rho_s C_s}\Delta t\right) T_{g,i}^{n} + \left(\frac{\Delta t}{(1-\varepsilon)\,\rho_s C_s}\right)\frac{P}{V_x} \tag{12}$$

To show the effect of an external heater, a resistive electrical heater with maximum power rating of 1150 W [21] is considered, and its influence on transient temperature behavior is analyzed. It is evident that transient temperature profiles and average bed temperature are improved (Figure 3), i. e. relatively faster warm-up is achieved compared to the case without an external heater. At the end of 7.6 minutes, the average bed temperature with heater is 920.9 K (1198 °F) compared to the maximum attainable temperature of 899.8 K (1160 °F) in the previous case (without heater). Note that these transient temperature profiles can be further improved by increasing the power rating of the heater, however, this depends on the availability of the heater and overall cost-effectiveness of the project.

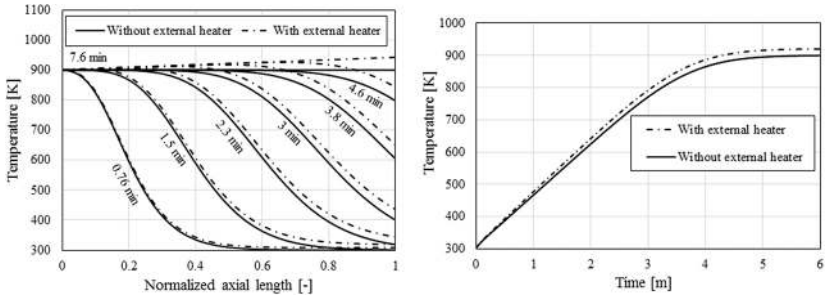

Figure 3: Comparison of solid temperature profiles without and with an external heater for constant temperature feed: (a) warm-up temperature, and (b) average temperature.

3 Mathematical model incorporating species conservation equations for CO oxidation

As exothermic chemical reaction happens at the surface of the catalyst, a source term is included in the energy conservation equation of the solid:

$$(1-\varepsilon)\,k_s\frac{\partial}{\partial x}\left(\frac{\partial T_s}{\partial x}\right)+a_s h\left(T_g-T_s\right)+a(x)H_{CO}R_{CO}=(1-\varepsilon)\,\rho_s C_s\frac{\partial T_s}{\partial t} \tag{13}$$

where, H_{CO} [J/mol] is the heat of reaction of CO oxidation, R_{CO} $\left[\text{mol}/\left(\text{m}^2\cdot\text{s}\right)\right]$ is the specific reaction rate of CO, and a_x $\left[\text{m}^2/\text{m}^3\right]$ is the catalytic surface area per unit reactor volume.

Upon comparing eqs. (2) and (13), it can be seen that there is an additional term present in eq. (13), which represents to the source term incorporating the heat generation due to CO oxidation. In the absence of this term, the maximum attainable temperature of the catalyst system is lesser or equal to the exhaust gas inlet temperature.

The bulk gas energy equation as reported in Section 2 is:

$$GC_{pg}\frac{\partial T_g}{\partial x}+a_s h\left(T_g-T_s\right)=0 \tag{14}$$

The bulk gas species equation is following [22]:

$$\varepsilon\frac{\partial \bar{c}_{g,j}}{\partial t}=-v\frac{\partial \bar{c}_{g,j}}{\partial x}-k_{m,j}a_s\left(\bar{c}_{g,j}-\bar{c}_{s,j}\right) \tag{15}$$

Where, $\bar{c}_{g,j}$ $\left[\text{mol}/\text{m}^3\right]$ and $\bar{c}_{s,j}$ $\left[\text{mol}/\text{m}^3\right]$ are concentrations of species j in bulk gas and surface phase, respectively. $k_{m,j}$ [m/s] is the diffusion mass transfer coefficient for species j, where j includes CO, O_2, and CO_2. a_s $\left[\text{m}^2/\text{m}^3\right]$ is the geometric surface area per unit reactor volume, and v [m/s] is the bulk gas velocity. In eq. (15), the term on the left-hand side describes the storage of species in the bulk gas, whereas the first term on the right-hand side describes the propagation of species in the bulk gas through the channel, and the second term describes the mass transfer of species from the bulk gas to the surface due to concentration difference. The species conservation equation for the surface is following:

$$\frac{\partial \bar{c}_{s,j}}{\partial t}=\frac{k_{m,j}a_s}{1-\varepsilon}\left(\bar{c}_{g,j}-\bar{c}_{s,j}\right)-\frac{a(x)R_j}{1-\varepsilon} \tag{16}$$

where, the term on the left-hand side represents to the storage of the species at the surface, the first term on the right-hand side describes the mass transfer of species between the surface and bulk gas, and the second term represents to the reaction at the surface. R_j $\left[mol/\left(m^2\cdot s\right)\right]$ is specific reaction rate of species j. The heat transfer coefficient h in eqs. (13) and (14) and the mass transfer coefficient $k_{m,j}$ in eqs. (15) and (16) are defined based on [22],

$$h=\frac{Nu_\infty k_g}{2R_h} \tag{17}$$

$$k_{m,j}=\frac{Sh_\infty D_{j,N_2}}{2R_h} \tag{18}$$

where, R_h $[m]$ is the hydraulic radius of the channel, Nu_∞ $[-]$ and Sh_∞ $[-]$ are limiting Nusselt number and Sherwood number, respectively. In a fully developed flow, Nusselt and Sherwood numbers approach a limiting value and becomes independent of axial direction. The values of both Nusselt and Sherwood numbers are obtained from fully developed laminar flow with constant wall heat flux as reported in Shah and London [23]. D_{j,N_2} $\left[\text{cm}^2/\text{s}\right]$ is the diffusivity of species j, and it is estimated by using the Slattery-Bird formula [24],

$$D_{j,N_2}=\left(p_{c,j}p_{c,N_2}\right)^{\frac{1}{3}}\left(T_{c,j}T_{c,N_2}\right)^{\frac{5}{12}}\left(\frac{1}{M_j}+\frac{1}{M_{N_2}}\right)^{\frac{1}{2}}\times 2.745\times 10^{-4}\times\left(\frac{T_s}{\sqrt{T_{c,j}T_{c,N_2}}}\right)^{1.823} \tag{19}$$

where, $p_{c,j}\,[atm]$ and $p_{c,N_2}\,[atm]$ are the critical pressures of species j and nitrogen, respectively. $T_{c,j}\,[K]$ is the critical temperature of species j, and $T_{c,N_2}\,[K]$ is the critical temperature of nitrogen. Similarly, $M_j\,[kg/mol]$ and $M_{N_2}\,[kg/mol]$ are the molecular weights of species j and nitrogen, respectively.

The reaction rate in eq. (16) is related to species j, where j = CO, O_2 and CO_2. In 1973, Voltz et al. [25] introduced a reaction model for the CO reaction in a gaseous blend of CO, C_3H_6, O_2, NO, CO_2 and N_2, by utilizing a multi-gas test bench with inhibition effects due to CO, C_3H_6, and NO. The following reaction mechanism was proposed:

$$R_{CO} = \frac{k_{CO} c_{CO} c_{O_2}}{G_1} \tag{20}$$

$$R_{C_3H_6} = \frac{k_{C_3H_6} c_{C_3H_6} c_{O_2}}{G_1} \tag{21}$$

where, $k_{CO}\left[mol/\left(m^2 \cdot s\right)\right]$ and $k_{C_3H_6}\left[mol/\left(m^2 \cdot s\right)\right]$ are defined as intrinsic rate constants for CO and C_3H_6 oxidation reactions based on catalyst volume. $G_1\,[-]$ is a resistance term for the inhibition effects of CO, C_3H_6 and NO. The expression for G_1 is:

$$G_1 = \left(1 + K_1 c_{CO} + K_2 c_{C_3H_6}\right)^2 \left(1 + K_3 c_{CO}^2 c_{C_3H_6}^2\right)\left(1 + K_4 c_{NO}^{0.7}\right) \tag{22}$$

where, $K_1\,[-]$ and$K_2\,[-]$ are defined as adsorption constants for CO and C_3H_6, respectively, $K_3\,[-]$ is the adsorption constant for combined effect of CO and C_3H_6, and $K_4\,[-]$ is the adsorption constant for NO. c_{O_2}, $c_{C_3H_6}$, c_{CO} and c_{NO} are surface species mole fractions of O_2, C_3H_6, CO and NO, respectively. It is to be noted that $\left(1 + K_1 c_{CO} + K_2 c_{C_3H_6}\right)^2$ in G_1 accounts for the inhibition effect due to CO and C_3H_6 [25], and $\left(1 + K_3 c_{CO}^2 c_{C_3H_6}^2\right)$ is required to fit the experimental data at higher concentrations of CO and C_3H_6. Furthermore, $\left(1 + K_4 c_{NO}^{0.7}\right)$ is the adsorption term for NO, which is one of the inhibiting species in the oxidation of CO and C_3H_6. Following this, Becker and Wei [26] proposed a model based on Voltz et al. [25] by considering adsorption of CO on Pt catalyst,

$$R_{CO} = \frac{k_{CO} c_{CO} c_{O_2}}{\left(1 + K_1 c_{CO}\right)^2} \tag{23}$$

However, in their analysis, the gaseous constituents at the inlet were only CO and O_2, which is far from any real case scenario. Oh and Cavendish [22] improved the reaction model proposed by Voltz et al. [25] and extended to two other species, namely CH_4 and H_2. The reaction model proposed by the authors for CO is:

$$R_{CO} = \frac{k_{CO} c_{CO} c_{O_2}}{G_2} \tag{24}$$

$$G_2 = T_s\left(1 + K_1 c_{CO} + K_2 c_{C_3H_6}\right)^2 \left(1 + K_3 c_{CO}^2 c_{C_3H_6}^2\right)\left(1 + K_4 c_{NO}^{0.7}\right) \tag{25}$$

The difference between Voltz et al. [25] and Oh and Cavendish [22] models are that the latter contained an extra term, "solid temperature" in its reaction inhibition mechanism. The addition of surface temperature $T_s\,[K]$ in the inhibition term can be explained in terms of surface coverage of CO. In 2003, Bourane and Binachi [27] observed that CO coverage on the active catalytic sites is nearly constant until 600 K, and decreases linearly with the increase in temperature. Prior to that, Rinnemo et al. [28] determined that the activation energy for CO oxidation increases with the decrease in CO coverage sites, which in turn makes oxidation process slow.

As modeling in catalytic converter is not an easy task and the reaction rate model poses a major challenge [29], in the present work, a simplified model is used based on Wei and Baker [20] and Oh and Cavendish [22]. In the model, solid temperature $[T_s]$ and inhibition effect due to CO are considered, and the inhibition parameters are not changed.

The global oxidation reaction happens over Pt-Al_2O_3 catalyst system is,

$$CO + \frac{1}{2}O_2 = CO_2 \tag{26}$$

$$R_{CO} = \frac{k_{CO} c_{CO} c_{O_2}}{G_{CO}} \tag{27}$$

$$G_{CO} = T_s (1 + K_{CO} c_{CO})^2 \tag{28}$$

where, $R_{CO}\left[mol/\left(m^2 \cdot s\right)\right]$ is the specific reaction rate for CO, $c_{CO}\,[-]$ and $c_{O_2}\,[-]$ are the mole fractions of CO and O_2 at the surface, $G_{CO}\,[K]$ is the inhibition activity due to CO, $K_{CO}\,[-]$ is the adsorption constant due to CO, $k_{CO}\left[mol \cdot K/\left(m^2 \cdot s\right)\right]$ is the rate constant for CO reaction, and $T_s\,[K]$ is the surface temperature.

The adsorption term in the inhibition is usually system insensitive, therefore, the values for activation energy and pre-exponential factor are taken as provided in [22, 25].

$$K_{CO} = 65.5 \exp\left(\frac{961}{T_s}\right) \tag{29}$$

$$G_{CO} = T_s \left(1 + 65.5 \exp\left(\frac{961}{T_s}\right) c_{CO}\right)^2 \tag{30}$$

$$k_{CO} = A \exp\left(\frac{-E_a}{R_u T_s}\right) \tag{31}$$

Note that $A\left[mol/\left(m^2 \cdot s\right)\right]$ is the pre-exponential parameter and $E_a\,[J/mol]$ is the activation energy, which are calibrated based on available experimental data. $R_u\,[J/\left(mol \cdot K\right)]$ is the universal gas constant. Based on the stoichiometric reaction, the reaction rates for O_2 and CO_2 in eq. (26) are,

$$R_{O_2} = 0.5 R_{CO} \tag{32}$$

$$R_{CO_2} = -R_{CO} \tag{33}$$

In the catalyst model, a number of boundary conditions are needed to solve the model, which are following,

$$T_s\,(x, 0) = T_{s0}(x) \tag{34}$$

$$T_g(0, t) = T_g^{in} \tag{35}$$

$$c_{g,j}(0, t) = c_{g,j}^{in} \tag{36}$$

$$c_{s,j}(0, t) = c_{g,j}^{in} \tag{37}$$

$$\frac{\partial T_s}{\partial x}|_{(0,t)} = \frac{\partial T_s}{\partial t}|_{(L,t)} = 0 \tag{38}$$

The discretization of surface phase energy equation, eq. (13), is based on the forward-time central-space (FTCS) method [30],

$$(1-\varepsilon)\,\rho_s C_s \frac{T_{s,i}^{n+1} - T_{s,i}^n}{\Delta t} = \left((1-\varepsilon)\,k_s \frac{T_{s,i+1}^n - 2T_{s,i}^n + T_{s,i-1}^n}{\Delta x^2} + a_s h\left(T_{g,i}^n - T_{s,i}^n\right) + a(x) H_{CO} R_{CO}\right) \tag{39}$$

The bulk gas energy and species equations, eqs. (14) and (15), are discretized by using the first-order difference method in order to ensure the accuracy and consistency for convergence of the solution along with fast computational speed.

$$G C_{pg} \frac{T_{g,i}^{n+1} - T_{g,i-1}^{n+1}}{\Delta x} + \frac{a_s h}{\varepsilon}\left(T_{g,i}^{n+1} - T_{s,i}^{n+1}\right) = 0 \tag{40}$$

$$v\frac{\bar{c}_{g,j,i}^{n+1}-\bar{c}_{g,j,i-1}^{n+1}}{\Delta x}-\frac{k_{m,j}^{n+1}a_s}{\varepsilon}\left(\bar{c}_{g,j,i}^{n+1}-\bar{c}_{s,j,i}^{n+1}\right)=0 \tag{41}$$

The surface phase species equation, eq. (16), is discretized implicitly in order to avoid the stiffness due to kinetic expression of the reaction term.

$$\frac{\bar{c}_{s,j,i}^{n+1}-\bar{c}_{s,j,i}^{n}}{\Delta t}=\frac{k_{m,j}^{n+1}a_s}{1-\varepsilon}\left(\bar{c}_{g,j,i}^{n+1}-\bar{c}_{s,j,i}^{n+1}\right)-\frac{a(x)R_j^{n+1}}{1-\varepsilon} \tag{42}$$

The time step used is;

$$\Delta t\leq\frac{2\rho_s C_s}{\frac{4k_s}{\Delta x^2}+\frac{ha_s}{1-\varepsilon}} \tag{43}$$

Note that the above time step is much more restricted than that of the time step reported in eq. (10), where the model is considered without chemical reaction.

3.1 Validation of the mathematical model for low CO concentration at the inlet

After validating the mathematical model for warm-up behavior and examining the influence of external heater on transient thermal response of the converter, the model is extended to incorporate the heat generation due to CO oxidation. Both high and low levels of CO concentration at the inlet are considered, and results are compared with available experimental data for low CO concentration from Pandya et al. [18] and for high CO concentration from Missy et al. [19] to ensure that the model works over a wide range of CO concentration at the inlet. It is worth notifying that the validation efforts in the present work incorporated the inlet concentrations (or mass fractions) of CO, O_2, and CO_2 as reported in the literature. The concentrations of other species, however, are ignored, and were replaced with nitrogen. The parameters of the three-way catalytic converter of 400 cells per square inch (CPSI) with wall thickness of 6.5 mil (1 mil = 25 µm) are provided in Table 2.

Table 2: Parameters for predicting light-off temperature for low concentration of CO at the inlet [18].

Symbol	Definition	Quantity
T_{s0}	Initial surface temperature	373 K
T_g^{in}	Inlet bulk gas temperature	350 K - 560 K
L	Length of the monolith	76.2 mm
D	Diameter of the monolith	25.4 mm
σ	Space velocity	50,000 h^{-1}
ρ_s	Solid density	410 kg/m^3
k_s	Thermal conductivity of solid	0.4 W/m/k
C_s	Specific heat capacity of solid	1130 kJ/kg/K

Exhaust gas specie [in ppm or % (v/v))] CO = 100 ppm); O_2 = 6 %; CO_2= 10 %, N_2 = balance

Both in Pandya et al. [18] and Missy et al. [19], experimental light-off curves were obtained by imposing the temperature ramps at the inlet of the oxidation catalysts. The experimental procedures were similar to Voltz et al. [25] utilizing synthetic gas test bench, and consisted of three major parts: the gas mixing unit, the gas pre-heater and reactor, and the gas analysers [18, 31]. The desired concentrations of different gaseous species were obtained by blending pure CO, C_3H_6, NO, H_2, CO_2 and N_2. The reactor was modeled using one-dimensional mathematical modeling approach, and was based on heterogeneous catalyst reactions in a single channel. While developing the kinetic model, Pandya et al. [18] considered the oxidation reactions of CO, C_3H_6, H_2 and NO, and reduction of NO by C_3H_6.

Figure 4 provides the comparison of CO conversion curves obtained using present model with both experimental and numerical results of Pandya et al. [18] for the low level of CO concentration (i. e. 100 ppm) at the inlet. It is worth notifying that experiments performed by Pandya et al. [18] utilized a synthetic gas test bench, and simulated the real exhaust gas scenario incorporating multi-species, i. e. CO, C_3H_6, NO, and H_2. Also, the model reported by Pandya et al [18] considered a set of multi-species global reaction rates for CO, C_3H_6, NO, and H_2, and included the inhibition effect due to CO as well as due to C_3H_6 and NO. Hence the model accounted eight coupled mass transfer equations (for CO, C_3H_6, NO, O_2) and four coupled reaction rates (CO,

C_3H_6, NO, O_2) along with two energy conservation equations (for bulk gas and solid) which is computationally difficult and expensive, and highly unstable. Moreover, as the reactions are sensitive to temperature and composition [32], this makes the model more complicated. It is reported that authors had 17 adjustable parameters for the global kinetic model [18]. However, the use of simplified reaction rate model, in the present work, helps in reducing the computational complexity as the focus is laid on CO conversion. Also, it can be seen (Figure 4) that the simplified model compares well with the CO conversion reported by Pandya et al. [18]. The adjustable parameters in the present simplified model, however, are only two, i. e. activation energy and Arrhenius coefficient.

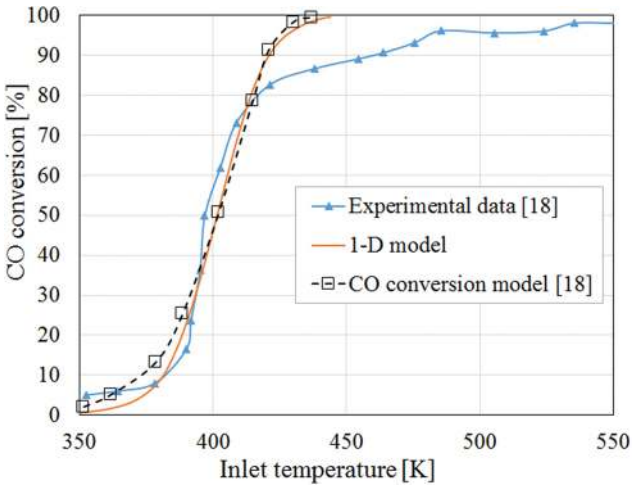

Figure 4: A comparison of CO conversion for low level of CO concentration at the inlet.

3.2 Validation of the mathematical model for high CO concentration at the inlet

Diesel engines operating under dual-fuel mode contains a high level of CO concentration in the exhaust [12]. To ensure a wide range of operation based on CO concentration at the inlet of the converter, the model is also validated with Missy et al. [19] having a high level of CO concentration at the inlet. Missy et al. [19] used a 400 CPSI ceramic converter with wall thickness of 6.5 mil, length of 0.1524 m and diameter of 0.1016 m. The mass flow rate of 95.2 kg/h was applied, and the temperature was increased slowly by 14.5 K/min from 380 K to 560 K. The conversion was assumed to be non-adiabatic, and modeling was carried out for a single channel.

Table 3 provides the parameters of the three-way catalytic converter of 400 CPSI and wall-thickness of 6.5 mil used for the modeling efforts.

Table 3: Parameters for predicting light-off temperature for high concentration of CO at the inlet [19].

Symbol	Definition	Quantity
T_{s0}	Initial surface temperature	373 K
T_g^{in}	Inlet bulk gas temperature	380 K - 560 K
L	Length of the monolith	152.4 mm
D	Diameter of the monolith	101.6 mm
G	mass flow rate of gas	95.2 kg/h
ρ_s	Solid density	410 kg/m^3
k_s	Thermal conductivity of solid	0.4 W/m/k
C_s	Specific heat capacity of solid	1130 kJ/kg/K

Exhaust gas specie (in mass fraction): CO = 0.00509 (4542.3 ppm); O_2 = 0.01 (10.2 %); CO_2 = 0.208, N_2 = balance

Figure 5 compares the conversion of CO utilizing the present model with available experimental data incorporating 4542 ppm of CO level at the inlet and the model data from [19]. As shown in Figure 5, the out of the present model compares well with the experimental data up to about 70 % of conversion, with relatively faster prediction beyond that compared to both experimental data and [19]. This is expected as the actual CO reaction is relatively slower due to the presence of propylene (C_3H_6) which has an inhibition effect on CO conversion rate [25], not considered in the present simplified model. As light-off temperature is defined based on 50 % con-

version of a gaseous species, this model is very useful for CO conversion through oxidation catalyst, particularly for dual-fuel engine operation with much less computational cost

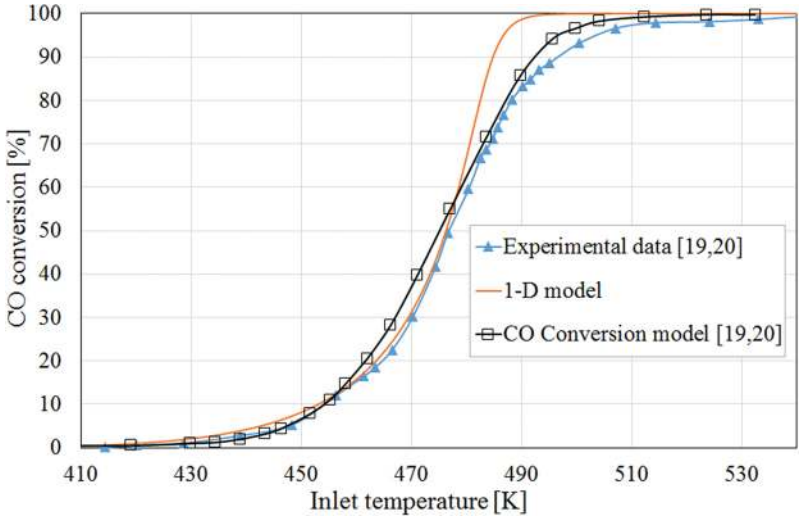

Figure 5: A comparison of CO conversion for high level of CO concentration at the inlet.

4 Conclusions

Over the past decades, the automotive emission norms have become more and more stringent to control the air pollution. Moreover, due to increase in fuel price along with ever growing demand for energy, the dual-fuel technology is becoming more popular. One of the promising candidates for dual-fuel technology is natural gas, owing to its low C/H ratio, and ability to reduce NO_x and PM simultaneously. However, during low and medium loads, CO and HC emissions are very high due to lower in-cylinder temperature and incomplete combustion. As most of the HC emission is methane under dual-fuel operating mode, the focus is laid upon CO oxidation. For this purpose, a simplified one-dimensional mathematical model is proposed based on underlying physical and chemical phenomena in a catalytic converter. At first, the model is developed without considering the heat generation due to chemical reactions, and is validated with Vardi and Biller [17] for the prediction of transient temperature profiles and average bed temperature of the converter for warm-up studies. In this stage, only energy conservation equations for both bulk gas and solid are utilized. This is particularly helpful for the analysis of converter producing little to no heat, for example, during the cold start of the engine. The average bed temperature of the converter is helpful for comparing different catalyst systems. During the cold start, as the exhaust gas temperature is lower than the light-off temperature of the converter, the warm-up behavior was improved by adding an external heater to the required volume as a source term.

After successful validation, the model is extended to incorporate the effect of chemical reaction due to CO oxidation with simplified reaction model. The inhibition effect due to CO is only considered, and corresponding species conversion equations are used. The reaction model is calibrated based on experimental data, and validation was performed for both high and low levels of CO concentration at the inlet with available experimental data. The model is particularly useful to study the conversion of CO through the oxidation catalyst for dual-fuel engine application, with high level of CO concentration under dual-fuel mode and low level of CO concentration under diesel only mode. The simplified reaction model reduced the computational complexity and difficulty associated with determining various parameters for exact mechanisms of CO reaction. Such analysis is particularly helpful for examining the light-off temperature with limited computational resources without depending upon other gaseous species. The model can also be extended by adding the oxidation reaction for C_3H_6 for studying the inhibition effect of C_3H_6 on CO conversion.

Acknowledgements

Financial support from Science and Engineering Research Board (SERB) of India through project number EMR/2016/007094 is gratefully acknowledged.

References

[1] Heck RM., Farrauto RJ, Gualiti ST. *Catalytic air pollution control- commercial technology*, 3rd ed. Hoboken: John Wiley & Sons, 2009.
[2] Karim GA.. *Dual-fuel diesel engines*, 1st ed. Boca Raton: Taylor & Francis Group, 2015.
[3] Koten H. Performance analysis of diesel engine within a multi-dimensional framework. J Thermal Eng. 2018;4;2075–82. DOI: 10.18186/journal-of-thermal-engineering.414153.
[4] Balenovic M. Modeling and model based control of a three-way catalytic converter PhD Thesis. [Eindhoven]: Eindhoven University of Technology; 2002, 174
[5] Iodice P, Senatore A. Exhaust emissions of new high-performance motorcycles in hot and cold conditions. Int J Environ Sci Technol. 2015;12;3133–44. DOI: 10.1007/s13762-014-0741-6.
[6] Iodice P, Langella G, Amoresano A. Ethanol in gasoline fuel blends: effect on fuel consumption and engine out emissions of SI engines in cold operating conditions. App Thermal Eng 2018;130;1081–9. DOI: 10.1016/j.applthermaleng.2017.11.090.
[7] Liu B, Hayes RE, Checkel MD, Zheng M, Mirosh E. Reversing flow catalytic converter for a natural gas/diesel dual fuel engine. Chem Eng Sci. 2001;56;2641–58. DOI: 10.1016/S0009-2509(00)00535-2.
[8] Gambino M, Cericola R, Corbo P. Carbonyl compounds and PAH emissions from CNG heavy-duty engine. J Eng Gas Turbines Power. 1993;115;747–9. DOI: 10.1115/1.2906769.
[9] Koten H, Yilmaz M, Gul MZ. Compressed biogas-diesel dual-fuel engine optimization study for ultralow emission. Adv Mech Eng. 2014. DOI: 10.1155/2014/571063.
[10] Karim GA. An examination of some measures for improving the performance of gas fuelled diesel engines at light load. SAE Technical Paper No. 912366. DOI: 10.4271/912366.
[11] Mittal M, Donahue R, Winnie P, Gillette A. Gaseous and soot emissions characteristics of a 15.2-liter compression ignition engine operated with natural gas and diesel pilot. J Energy Inst. 2014;10;63–9. DOI: 10.1016/j.joei.2014.09.003.
[12] Majewski WA, Khair MK.. *Diesel emissions and their control*. Warrendale: SAE International, 2006.
[13] Depcik C, Assanis D.. One-dimensional automotive catalyst modeling. Prog Energy Combust Sci. 2005;31;308–69. DOI: 10.1016/j.pecs.2005.08.001.
[14] Kuo JCW, Morgan CR, Lassen HG.. SAE Technical Paper No. 710289 Mathematical modeling of CO and HC catalytic converter systems. DOI: 10.4271/710289.
[15] Chauhan S, Kumar D, Srivastava VK. Modeling catalytic combustion of methane during the warm-up period of the converter. Chem Prod Proc Mod. 2009;4;1–15. DOI: 10.2202/1934-2659.1278.
[16] Indian Emission Regulation Booklet. ARAI (automotive research association of India): OBD threshold for BS VI vehicles manufactured on or after 1 April 2020. https://www.araiindia.com/pdf/Indian_Emission_Regulation_Booklet.pdf (accessed on 25th August, 2018)
[17] Vardi J, Biller WF. Thermal behavior of an exhaust gas catalytic converter. I and EC Proc Des Dev. 1968;7;83–90. DOI: 10.1021/i260025a017.
[18] Pandya A, Mmbaga J, Hayes RE, Hauptmann W, Votsmeier M. Global kinetic model and parameter optimization for a diesel oxidation catalyst. Top Catal. 2009;52(13–20);1929–33. DOI: 10.1007/s11244-009-9361-7.
[19] Missy S, Thams J, Bollig M, Tatschl R, Wanker R, Bachler G. Computergestütze optimierung des abgasnachbehandlungssystems für den neuen 1.8-l-valvetronic-motor von BMW [Computer-aided optimisation of the exhaust gas aftertreatment system of the new BMW 1.8-litre valvetronic engine]. *MTZ Motortech Z*. 2002;63:1203–12. DOI: 10.1007/BF03226607.German.
[20] Wurzenberger JC, Peters BJ. Catalytic converters in a 1d cycle simulation code considering 3d behaviour. SAE Technical Paper No. 2003-01-1002. DOI: 10.4271/2003-01-1002.
[21] Oh SH, Bissett EJ, Battiston PA. Mathematical modeling of electrically heated monolith converters: model formulation, numerical methods, and experimental verification. Ind Eng Chem Res. 1993;32;1560–7. DOI: 10.1021/ie00020a005.
[22] Oh SH, Cavendish JC. Transients of monolithic catalytic converters: response to step changes in feedstream temperature as related to controlling automobile emissions. Ind Eng Chem Prod Res Dev. 1982;22;29–37. DOI: 10.1021/i300005a006.
[23] Shah RK, London AL. Laminar flow forced convection heat transfer and flow friction straight and curved ducts – A summary of analytic solutions. Dept. of Mechanical Eng., Stanford University, Stanford (CA), 1971, 280. Technical Report No. 75. Contract No. 225 (91)[NR-090-342] for Office of Naval Research.
[24] Bird RB, Stewart WE, Lightfoot EN.. *Transport phenomena*. New York: John Wiley. Reprint 1960.
[25] Voltz SE, Morgan CR, Liederman D, Jacob SM.. Kinetic study of carbon monoxide and propylene oxidation on platinum catalysts. Ind Eng Chem Prod Res Dev. 1973;12;294–01. DOI: 10.1021/i360048a006.
[26] Becker ER, Wei J. Nonuniform distribution of catalysts on supports. I. Bimolecular langmuir reactions. J Catal. 1977;46;365–71. DOI: 10.1016/0021-9517(77)90220-2.
[27] Bourane A, Bianchi D. Heats of adsorption of the linear CO species on Pt/Al_2O_3 using infrared spectroscopy: impact of the Pt dispersion. J Catal. 2003;218;447–52. DOI: 10.1016/S0021-9517(02)00183-5.
[28] Rinnemo M, Kulginov D, Johansson S, Wong KL, Zhdanov VP, Kasemo B. Catalytic ignition in the $CO-O_2$ reaction on platinum: experiment and simulations. Surf Sci. 1997;376;297–9. DOI: 10.1016/S0039-6028(96)01572-5.
[29] Chauhan S, Srivastava VK. Modeling the effect of temperature on propylene conversion during warm-up in a monolithic converter. Chem Prod Proc Mod. 2008;3;1–12. DOI: 10.2202/1934-2659.1232.
[30] Loya S, Depcik C. Modifying the classical one-dimensional catalyst model to include axial conduction and diffusion. J Eng Gas Turbines Power. 2013;135;091506–1–8. DOI: 10.1115/1.4024421.
[31] Salomons S, Votsmeier M, Hayes RE, Drochner A, Vogel H, Gieshof J. CO and H_2 oxidation on a platinum monolith diesel oxidation catalyst. Cat Today. 2006;117;491–7. DOI: 10.1016/j.cattod.2006.06.001
[32] Rao SK, Imam R, Ramanathan K, Pushpavanam S. Sensitivity analysis and kinetic parameter estimation in a three way catalytic converter. Ind Eng Chem Res. 2009;48;3779–90. DOI: 10.1021/ie801244w.